A Critical Cross-Examination on Load-Balancing Transformers for Distribution Systems

D. Ahmadi, M. Tavakoli Bina, *Senior Member, IEEE*, and M. Golkar

***Abstract*—A load balancing transformer (LBT) has already been suggested for improving the unbalance of three-phase primary currents. Each phase includes one extra pair of coupling windings in addition to the usual primary and secondary windings. Two coupling windings, located on two different phases, are made in series, where the resulting circuit is then reversely paralleled with the secondary winding placed on the third phase. Under unbalanced conditions, the load currents are distributed between the coupling and secondary windings that are supplied through different primary phases. This paper proposes a method in order to define all possible LBTs, which paves the way to cross-examine and select the best connections of windings for the LBT. Starting from the original LBT, it is shown that the best LBT is practically connected, such as a zig-zag winding. Then, a novel idea is suggested in which a controller and some four-quadrant semiconductor switches contribute to the improvement of the performance of the LBT. These switches should control the amount of current transfer from one phase to another. A combinatorial selection problem is arranged to find the best way of switching modulation. Both simulations and experimental works (using a designed 12-kVA laboratory prototype) verify the studied examination and proposals, showing the switch-mode zig-zag LBT as having the best performance.**

***Index Terms*—Load-balancing transformer, optimized switching, unbalanced condition.**

NOMENCLATURE

$\mathbf{CV}$	Configuration vector.
$\beta_1, \beta_2, \beta_3$	Coefficients of the $\mathbf{CV}$.
$\lambda_1, \lambda_2, \lambda_3$	Elements of the connection matrix.
$\mathbf{i}, \mathbf{j}, \mathbf{k}$	Three per-unit phasors sequentially having 120° phase difference.
I_{P0}, I_{P-}, I_{P+}	Zero, negative, and positive sequence of the primary currents.
I_{S1}, I_{S2}, I_{S3}	Secondary load currents.
$\mathbf{Z}$	Transformation matrix that connects primary and secondary currents.
C_1, C_2, C_3	Switching values related to the six coupling windings of a single-stage switch-mode LBT.
S_1, S_2, S_3	Switching values related to the three secondary windings of a single-stage switch-mode LBT.
$C_{11}, C_{12}, C_{21}, C_{22}, C_{31}, C_{32}$	Switching values related to the twelve coupling windings of a two-stage switch-mode LBT.
$s_{11}, s_{12}, s_{21}, s_{22}, s_{31}, s_{32}$	Switching values related to the six secondary windings of a two-stage switch-mode LBT.
RC	Released capacity by the LBT in percent.
CUF	Current unbalance factor.
Mag	Magnitude of zero and negative unbalance factor.
NW_P, NW_S, NW_C	Number of windings assigned to the primary, secondary, and coupling.
NT_P, NT_S, NT_C	Number of turns assigned to the primary, secondary, and coupling windings.

Manuscript received November 22, 2009; revised March 02, 2010. First published June 10, 2010; current version published June 23, 2010. Paper no. TPWRD-00862-2009.

The authors are with the Electrical Engineering Faculty, K. N. Toosi University of Technology, Tehran 16314, Iran. (e-mail: tavakoli@kntu.ac.ir)

Color versions of one or more of the figures in this paper are available online at http://ieeexplore.ieee.org.

Digital Object Identifier 10.1109/TPWRD.2010.2048222

I. INTRODUCTION

UNBALANCED condition is coined with the operation of distribution networks. It may cause one phase of the substation transformer (20 kV/400 V) to reach its rated value earlier, while the other two phases operate well below their nominal ratings. Hence, the capacity of the substation transformer has to be increased, which raises the investment cost along with the variable cost of substation transformers because of the unused available capacity. Unbalancing in distribution networks also increases the power losses of the conductors, creates zero-sequence voltage drop on the neutral wire, as well as voltage drop across the network.

It is noticeable that the variation of single-phase loads can be regarded as a fuzzy-random behavior across the distribution network [1]. Also, since single-phase loads are not uniformly distributed, it is almost inconceivable to manage a complete

balance for a distribution network. However, some techniques have been previously proposed to reduce the unbalance and its side effects. One approach is the usage of static compensators in order to modify the network admittances [2], [3]. Single-phase loads can be switched ON/OFF in a way that constantly changes the network admittances. While this method could be expensive for distribution networks, it would be practically hard to achieve too.

Synchronous condensers and induction motors can also absorb negative components of current as rotating balancers. This approach might be expensive due to the high cost and power losses. The use of flexible ac transmission (FACTS) controllers is another technique that recently has made prominent theoretical progress [4]–[8]. The employment of these devices relies on advances of technology in order to deal with technical issues, such as harmonics, efficiency, and implementation process. Also, active filters [9]–[14] or a combination of FACTS controllers and active filters [13] have been proposed which are expensive that have complications in design, control, and implementation. In the meantime, all of these devices are unable to supply energy to the load unless the required energy is supplied by an external source into these static compensators.

This paper proposes some modifications on the structure of the originally suggested load balancing transformer (LBT) in order to improve the balancing performance. Suggestions include a number of additional coupling windings along with a number of four-quadrant switches in series with those coupling windings. Hence, a controller is designed to examine the best switching combination. In fact, a combinatorial optimization program will manage this task by looking for the most desirable balanced situation for the LBT. Both the balancing transformer and the suggested switches along with the controller are simulated with MATLAB. Simulations confirm that the modified switch-mode balancing transformer introduces a better balancing outcome compared to the original LBT. Furthermore, a modulated 12-kVA LBT (including 12 switches) was designed and developed to examine the performance of the modified LBT. Three AVRATMEGA8 monitors the unbalanced current, and an AVRATMEGA16 microcontroller was used to manage the selection of the best switching status. Experimental results verify the capability of the switch-mode best LBT over the earlier cross-examined versions in terms of tackling the load unbalance. In brief, simulations and experiments show that the final suggestion, the switch-mode best LBT, offers several advantages such as the lowest unbalance of the primary currents, the highest released capacity for the distribution transformer, lower cost, weight, and volume compared to the other kinds of the LBT, and capable of simultaneous mitigation of the negative- and zero-sequence components.

II. Background Discussions and Analysis

A special distribution transformer is suggested in [15] to balance the source-end current of an unbalanced load. In this transformer, the three-phase secondary windings are connected together in a special way such as the topology shown in Fig. 1. This connection is arranged in a way that the secondary of each phase consists of three windings; for example, a winding on column T1 (A) is in series with a winding on column T2 (E),

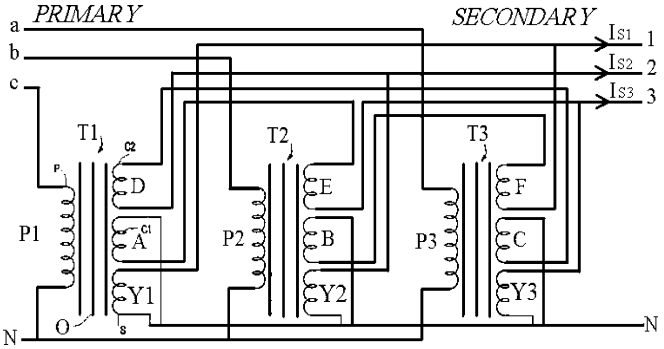

Fig. 1. Original LBT.

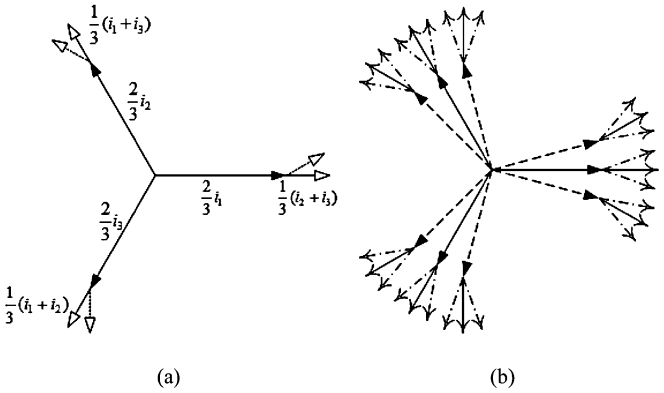

Fig. 2. Current distribution for the ordinary load balancing transformer. (a) A specific current distribution. (b) Various possible distributions.

where the resultant combination is inversely paralleled with a winding on column T3 (Y3). In this kind of transformer, two-thirds of the load current flow through one winding and the remaining one-third through a set of two series windings. For example, according to Fig. 1, two-thirds of the load current that is connected to point 3 of the secondary side are supplied by winding Y3 and one-third by the two windings A and E. Hence, the load current at each phase is not equally supplied from three primary phases [shown in Fig. 2(a) and (b)].

A. Expansion of the Idea of the LBT

The proposed configuration of Fig. 1 ([15]) can be further generalized. Here, a general procedure is suggested to create new configurations for the LBT. Assume three windings are located on three separate arms of the transformer. Furthermore, let us consider three per-unit phasors $\mathbf{i}, \mathbf{j}$, and $\mathbf{k}$ sequentially having 120° phase difference. Then, a linear combination of these vectors can be formed as the configuration vector $(\mathbf{CV})$ as the secondary-side load voltage

$$\mathbf{CV} = \beta_1 \mathbf{i} + \beta_2 \mathbf{j} + \beta_3 \mathbf{k} \tag{1}$$

where three real parameters $[\beta_1, \beta_2, \beta_3]$ represent the configuration vector. Hence, the number of required windings for each $\mathbf{CV}$ is smaller than or equal to three. Since further $\mathbf{CV}$s can also be paralleled with the available $\mathbf{CV}$, the larger the number of $\mathbf{CV}$s, the larger the number of the necessary secondary windings. For example, the original LBT includes two $\mathbf{CV}$s; the first $\mathbf{CV}$ is represented by $[0, -1, -1]$, paralleled with the second

CV described by [1, 0, 0]. The number of nonzero elements of all **CV**s shows the number of the needed secondary windings for each phase; here, 3×3 gives nine secondary windings for three phases in total.

Further, it is noticeable that three-phase systems need three different phasors having the same magnitudes along with identical 120° phase differences for each selected **CV** in order to be regarded as an acceptable configuration for the balancing transformer. Fig. 3(a) and (b) shows 15 different possible **CV**s (listed in the Appendix). Nevertheless, these acceptable configurations should be evaluated based on their eventual balancing performances, their costs, weights, and dimensions. Here, four possible **CV**s among many possible designs are listed (the Appendix lists other CVs related to Fig. 3(a) and (b)) as

$$\text{Type 1}: \begin{cases} [0,-1,-1]\|[1,0,0] \text{ or } -(\mathbf{j}+\mathbf{k})\|\mathbf{i} \\ [-1,0,-1]\|[0,1,0] \text{ or } -(\mathbf{i}+\mathbf{k})\|\mathbf{j} \\ [-1,-1,0]\|[0,0,1] \text{ or } -(\mathbf{i}+\mathbf{j})\|\mathbf{k} \end{cases} \tag{2}$$

$$\text{Type 2}: \begin{cases} [\sqrt{3},1,-1] \text{ or } (\sqrt{3}\mathbf{i}+\mathbf{j}-\mathbf{k}) \\ [1,-1,\sqrt{3}] \text{ or } (\sqrt{3}\mathbf{k}+\mathbf{i}-\mathbf{j}) \\ [-1,\sqrt{3},1] \text{ or } (\sqrt{3}\mathbf{j}+\mathbf{k}-\mathbf{i}) \end{cases} \tag{3}$$

$$\text{Type 3}: \begin{cases} [0,1,-1] \text{ or } (\mathbf{j}-\mathbf{k}) \\ [1,-1,0] \text{ or } (\mathbf{i}-\mathbf{j}) \\ [-1,0,1] \text{ or } (\mathbf{k}-\mathbf{i}) \end{cases} \tag{4}$$

$$\text{Type 4}: \begin{cases} [\sqrt{3},1,-1]\|[1,0,-2] \text{ or } (\sqrt{3}\mathbf{i}+\mathbf{j}-\mathbf{k})\|(\mathbf{i}-2\mathbf{k}) \\ [1,-1,\sqrt{3}]\|[0,-2,1] \text{ or } (\sqrt{3}\mathbf{k}+\mathbf{i}-\mathbf{j})\|(\mathbf{k}-2\mathbf{j}) \\ [-1,\sqrt{3},1]\|[-2,1,0] \text{ or } (\sqrt{3}\mathbf{j}+\mathbf{k}-\mathbf{i})\|(\mathbf{j}-2\mathbf{i}) \end{cases} \tag{5}$$

Then, the relationship between the primary-side current vector $(\mathbf{i_P})$ and the secondary-side current $(\mathbf{i_S})$ for each choice can be worked out as follows:

$$\mathbf{i_P} = \mathbf{Z}\mathbf{i_S} \tag{6}$$

where the transformation matrix $\mathbf{Z}$ relates the three-phase primary currents $(\mathbf{i}_\mathrm{P})$ to those of the secondary $(\mathbf{i}_\mathrm{S})$. The matrix $\mathbf{Z}$ was calculated for connecting configurations shown by (2)–(5) as follows:

$$\begin{cases} Z_{(\text{Connection type}(1))} = \frac{1}{3}\begin{bmatrix} 2 & -1 & -1 \\ -1 & 2 & -1 \\ -1 & -1 & 2 \end{bmatrix} \\ Z_{(\text{Connection type}(2))} = \begin{bmatrix} 0.57 & 1 & -1 \\ -1 & 0.57 & 1 \\ 1 & -1 & 0.57 \end{bmatrix} \\ Z_{(\text{Connection type}(3))} = \begin{bmatrix} -1 & 0 & 1 \\ 1 & -1 & 0 \\ 0 & 1 & -1 \end{bmatrix} \\ Z_{(\text{Connection type}(4))} = \begin{bmatrix} 1.41 & -1.43 & 0.5625 \\ 0.5625 & 1.41 & -1.43 \\ -1.43 & 0.5625 & 1.41 \end{bmatrix} \end{cases}. \tag{7}$$

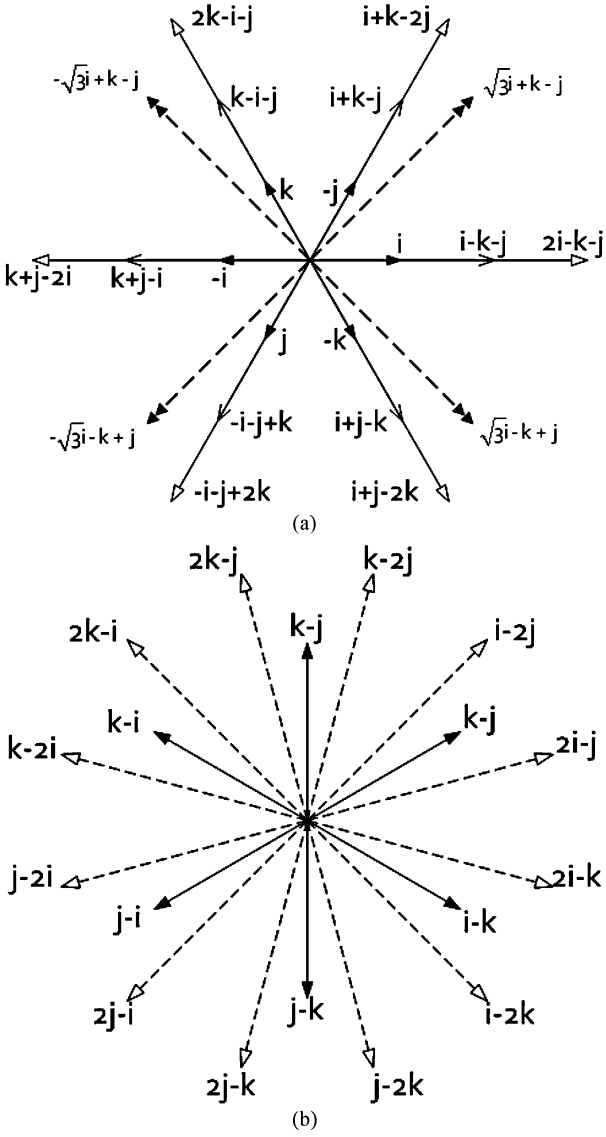

Fig. 3. (a)–(b) Several possible connection ways (**CV**s) for producing LBT.

The Appendix shows the remaining 11 connecting configurations, where some of them require larger weights and volumes. Also, all 15 combinations shown in Fig. 3 were simulated by SIMULINK; comparing their resulting primary currents in terms of their balancing condition singles out the best design for the LBT as shown in Fig. 4. Interestingly, the secondary winding of the best design for the LBT is basically the same as that of a zig-zag winding. This conclusion is obtained based on the suggested general configuration for the LBT, where here it is analytically shown as well.

Here, it is shown mathematically that the resulting LBT of Fig. 4 is the best among all possible **CV**s. To show this, assume the relationship between components in the matrix $\mathbf{Z}$ for each choice can be worked out as follows:

$$\mathbf{Z}_{(\text{Connection})} = \begin{bmatrix} \lambda_1 & \lambda_3 & \lambda_2 \\ \lambda_2 & \lambda_1 & \lambda_3 \\ \lambda_3 & \lambda_2 & \lambda_1 \end{bmatrix}. \tag{8}$$

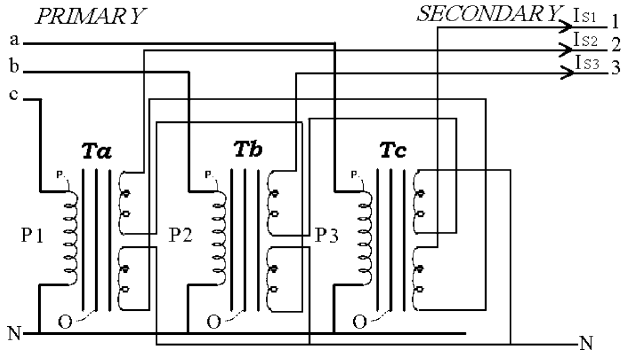

Fig. 4. Best LBT.

Also, let the secondary currents I_{S1}, I_{S2}, I_{S3} in (6) relate to the well-known symmetrical components such as ($\alpha = e^{j120^\circ}$) [16]–[18]

$$\begin{bmatrix} I_{P0} \\ I_{P-} \\ I_{P+} \end{bmatrix} = \frac{1}{3} \begin{bmatrix} 1 & 1 & 1 \\ 1 & \alpha^2 & \alpha \\ 1 & \alpha & \alpha^2 \end{bmatrix} \mathbf{Z} \begin{bmatrix} I_{S1} \\ I_{S2} \\ I_{S3} \end{bmatrix} \tag{9}$$

where I_{P0}, I_{P-}, I_{P+} are zero–, negative–, and positive-sequence currents related to the three-phase primary currents I_{Pa}, I_{Pb}, I_{Pc}. Substituting (8) in (9) and assuming $A = \lambda_2/\lambda_1$ and $B = \lambda_3/\lambda_1$ result in

$$\begin{bmatrix} I_{P0} \\ I_{P-} \\ I_{P+} \end{bmatrix} = \left(\begin{bmatrix} 1+A+B & 1+A+B & 1+A+B \\ 1-A & B-1 & A-B \\ 1-B & B-A & A-1 \end{bmatrix} + \alpha \begin{bmatrix} 0 & 0 & 0 \\ B-A & A-1 & 1-B \\ A-B & 1-A & B-1 \end{bmatrix} \right) \begin{bmatrix} I_{s1} \\ I_{s2} \\ I_{s3} \end{bmatrix}. \tag{10}$$

Then, partial differentiations of $|I_{P-}|$ with respect to A and B are set to zero to achieve the minimum value for $|I_{P-}|$. Simplifying the equations will eventually result in $|A - B| = 1$. At the same time, according to (10), $|I_{P0}|$ will be zero, when $A + B + 1 = 0$. The combination of these two outcomes suggests two possibilities for A and B as shown in Table I.

Hence, considering either the first or the second row ($\lambda_2 = \lambda_1$ and $\lambda_3 = 0$), the resulting impedance matrix matches the third connection type presented in (7) that matches Fig. 4. Therefore, Fig. 4 is the best connection arrangement for windings of the LBT in line with the performed simulations.

TABLE I
POSSIBLE VALUES FOR A AND B

A	B
−1	0
0	−1

To compare the original LBT (see Fig. 1) with the best LBT (see Fig. 4), the resulting relationship (9) can be worked out for the two cases introduced by (2) and (4) as follows:

$$\begin{cases} \begin{bmatrix} I_{P0} \\ I_{P-} \\ I_{P+} \end{bmatrix}_{\text{Connection type (1)}} = \frac{1}{3} \begin{bmatrix} 0 & 0 & 0 \\ 1 & -0.5 - j0.866 & -0.5 + j0.866 \\ 1 & -0.5 + j0.866 & -0.5 - j0.866 \end{bmatrix} \mathbf{I}_S \\ \begin{bmatrix} I_{P0} \\ I_{P-} \\ I_{P+} \end{bmatrix}_{\text{Connection type (3)}} = \frac{1}{3} \begin{bmatrix} 0 & 0 & 0 \\ 1 & -0.5 - j0.866 & -0.5 + j0.866 \\ 0.5 - j0.866 & 0.5 + j0.866 & -1 \end{bmatrix} \mathbf{I}_S \end{cases}. \tag{11}$$

Clearly, (11), shown at the bottom of the page, indicates that some connecting structures (such as (2) and (4)), unlike other possible connections, have the advantage of transferring no zero-sequence current from the load to the primary side of the transformer. This also shows that the resulting best LBT performs like the original LBT in terms of zero-sequence unbalance, providing a slightly better current unbalance factor as well as identical released capacity as shown in Section V. However, the cost, weight, and volume of the best LBTs are less than those of the original LBT because of fewer windings for the optimal LBT. The next question is whether the performance of the best LBT can be improved further. The following section studies a switched-mode proposal to address this question.

III. SUGGESTING MODIFICATIONS TO THE LBT

The LBT can compensate the unbalance of grid networks, lowering the unusable capacity of the distribution transformer. This freed capacity of the distribution transformer can then be made available for selling to the consumers. One disadvantage of these transformers, however, is that the level of unbalance distribution of primary currents is only decided by the inflexible distribution of secondary load currents as shown typically by the constant connecting matrices in (7). This issue will not only lower the performance of the balancing transformer, it can also accentuate the current unbalance of the primary side. Thus, to distribute the currents among the three primary phases more evenly, a switch-mode proposal is presented here to enhance the flexibility in selecting the path of secondary currents. It is noticeable that each secondary phase includes two parallel branches, as shown in the equivalent circuit of Fig. 5, which essentially makes both branches have identical voltage magnitudes and phase angles.

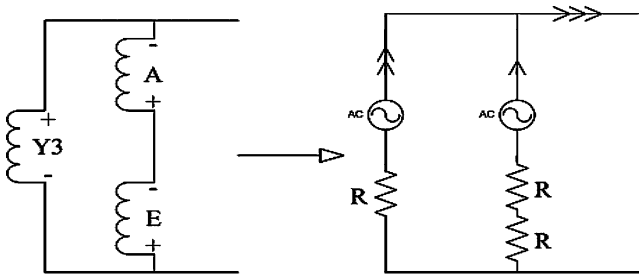

Fig. 5. Equivalent circuit of the LBT for each phase.

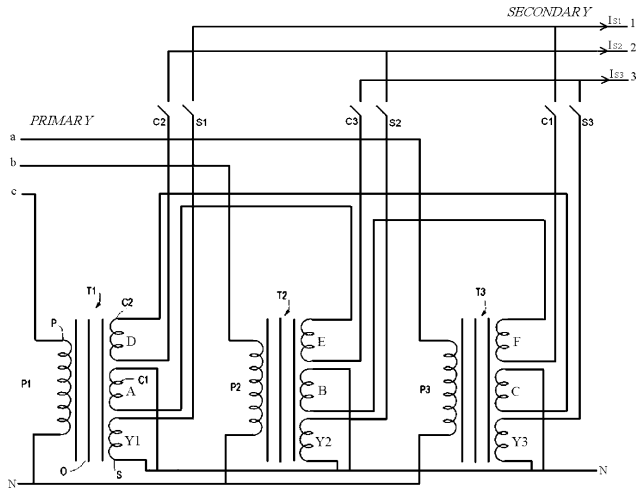

Fig. 6. Suggested switch-mode topology including six additional switches.

A. Modified LBT

To control the primary currents, the structure of the LBT is modified, as shown in Fig. 6 by adding two switches to each secondary phase. Considering Fig. 5, the inclusion of one switch per branch (both secondary winding and series coupling winding) needs two switches per phase. In total, six switches are responsible for the regulation of primary currents. While two switches of each phase can be turned ON simultaneously, at least one branch must supply current to the load. Otherwise, the continuity of the load current will not be satisfied in practice (i.e., simultaneous turnoff is not allowed for the two switches of each phase).

Meanwhile, turning one switch off would lead to the disconnection of either the series coupling windings or the secondary winding; this implies a change in the distribution of load currents among the primary phases of the LBT. Then, the problem is narrowed down to the selection of the best possible switching states in performing the balancing task of the transformer.

1) Analysis and Operation of the Modified LBT: Fig. 6 shows that three switches s_1, s_2, and s_3 connect the secondary windings $\mathrm{Y}_1, \mathrm{Y}_2$, and Y_3 to the three phases numbered as 1, 2, and 3. Also, coupling windings B and F are connected through the switch C_1 to phase 1, C and D through the switch C_2 to phase 2; finally, A and E are through the switch C_3 to phase 3. Considering phase 1, when the switch C_1 is turned ON and s_1 is OFF, the secondary current at phase 1 is supplied through the coupling windings B and F by the primary phases a and b. When the two switches C_1 and s_1 are turned OFF and ON, respectively, then the secondary current at phase 1 is totally supplied by the primary phase c. At last, when switches C_1 and s_1 are turned ON, two-thirds of the secondary current at phase 1 are supplied by primary phase c, and the remaining one-third is through B and F by the other two primary phases a and b (see Table II).

TABLE II
ALL COMBINATIONS OF THE TWO SWITCHES PER PHASE

C_1	S_1	$\mathbf{I_{Pa}}$	$\mathbf{I_{Pb}}$	$\mathbf{I_{Pc}}$
1	1	$-0.33i_{s1}$	$-0.33i_{s1}$	$0.66i_{s1}$
0	1	0	0	i_{s1}
1	0	$-i_{s1}$	$-i_{s1}$	0
0	0	Not allowed		

Hence, considering possible switching states for the other two phases, primary and secondary currents can be described by using the following relationship:

$$\begin{bmatrix} I_{Pa} \\ I_{Pb} \\ I_{Pc} \end{bmatrix} = \begin{bmatrix} k_1 - 1 & k_2 - 1 & k_3 \\ k_1 - 1 & k_2 & k_3 - 1 \\ k_1 & k_2 - 1 & k_3 - 1 \end{bmatrix} \begin{bmatrix} I_{S1} \\ I_{S2} \\ I_{S3} \end{bmatrix} \tag{12}$$

where three values k_1, k_2, and k_3 can be given as follows:

$$\begin{cases} k_1 = \frac{2s_1}{2+C_1} \\ k_2 = \frac{2s_2}{2+C_2} \\ k_3 = \frac{2s_3}{2+C_3} \end{cases} \tag{13}$$

where the six switching states s_1, s_2, s_3, C_1, C_2, and C_3 are equal to 1 when they are turned ON, and 0 for OFF position. It is noticeable that (12) still holds for the original LBT if $k_1 = k_2 = k_3 = 2/3$ (see Fig. 4).

Since there are three possible switching states for the two switches of each phase in practice, 27 possible switching statuses are available for a three-phase combination in total. A real-time control program can be arranged to perform the selection of the best switching status based on the load condition. Thus, samples of the load currents are taken and supplied to a microcontroller. Then, based on a preset objective function (e.g., lowering primary current unbalance percent, power losses minimization, or the used capacity maximization), all 27 switching states are examined and the most suitable switching combination is selected. This algorithm would start by selecting another switching status whenever the differential peak of the three-phase currents during two consecutive samples goes beyond a certain adjustable level. It can also be adjusted to repeat the whole algorithm every 5 min (adjustable) in the case that the load varies smoothly (the daily load profile of distribution feeders usually changes smoothly).

In brief, the advantages obtained from including switches can be named as having control of the distribution of currents among the three primary phases along with affecting the released capacity by the LBT (see Tables IV and V, which summarize the outcomes of simulations and experiments).

B. Generalization of the Proposed Modification to the Multistage LBT

Another suggestion could be the increase of the number of secondary or coupling windings. Thus, the number of switches

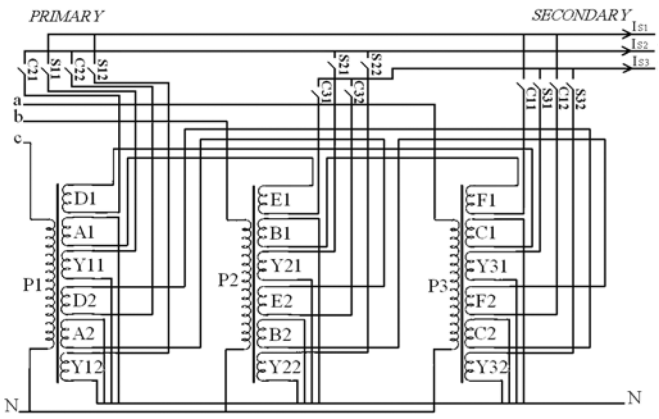

Fig. 7. Generalized switch-mode topology proposed for the LBT.

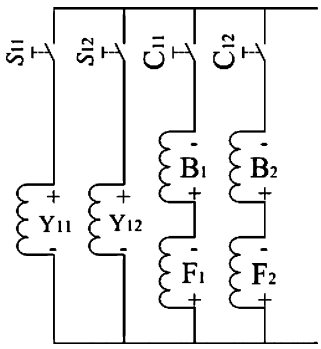

Fig. 8. Equivalent circuit of the two-stage switch-mode LBT for each phase.

per phase can be increased, arranging a significant number of possible switching states for the controller. However, it is noticeable that increasing the number of windings and switches affects the cost of the transformer as well as the protection and maintenance of the LBT. Fig. 7 shows a typical two-stage switch-mode LBT. Six switches $s_{11}, s_{12}, s_{21}, s_{22}, s_{31}$, and s_{32} connect six secondary windings $\mathrm{Y}_{11}, \mathrm{Y}_{21}, \mathrm{Y}_{12}, \mathrm{Y}_{22}, \mathrm{Y}_{31}$, and Y_{32} to three phases numbered from 1 to 3, respectively. Also, six switches $C_{11}, C_{12}, C_{21}, C_{22}, C_{31}, C_{32}$ connect six set of two coupling windings in series $(\mathrm{B}_1, \mathrm{F}_1)$, $(\mathrm{B}_2, \mathrm{F}_2)$, $(\mathrm{C}_1, \mathrm{D}_1,)$ $(\mathrm{C}_2, \mathrm{D}_2,)$ $(\mathrm{A}_1, \mathrm{E}_1)$, and $(\mathrm{A}_2, \mathrm{E}_2)$ to three phases numbered from 1 to 3, respectively.

An equivalent circuit for phase 1 of the two-stage LBT in Fig. 7 is shown in Fig. 8. There are different switching combinations for controlling the unbalance of the primary-side currents. For example, when only the switch C_{11} is turned ON, the secondary current at phase 1 is supplied through the series coupling windings $(\mathrm{B}_1, \mathrm{F}_1)$, balancing this secondary flux through the primary currents in phases a and b. When only the switch s_{12} is ON, then the secondary current at phase 1 is totally supplied by the primary phase c. When two switches (either C_{11} or C_{12}) and (either S_{11} or S_{12}) are turned ON, two-thirds of the secondary current at phase 1 is supplied by primary phase c, and the remaining one-third are through primary phases a and b. Details of all possible switching combinations and their related primary and secondary currents are listed in Table III.

TABLE III
POSSIBLE COMBINATIONS OF THE FOUR SWITCHES PER PHASE IN FIG. 7

C_{11}	C_{12}	s_{11}	s_{12}	$\mathbf{I_{Pa}}$	$\mathbf{I_{Pb}}$	$\mathbf{I_{Pc}}$
1	1	1	1	-0.33 i_{sl}	-0.33 i_{sl}	0.66 i_{sl}
1	0	1	0	-0.33 i_{sl}	-0.33 i_{sl}	0.66 i_{sl}
1	0	0	1	-0.33 i_{sl}	-0.33 i_{sl}	0.66 i_{sl}
0	1	0	1	-0.33 i_{sl}	-0.33 i_{sl}	0.66 i_{sl}
0	1	1	0	-0.33 i_{sl}	-0.33 i_{sl}	0.66 i_{sl}
1	1	1	0	-0.5 i_{sl}	-0.5 i_{sl}	0.5 i_{sl}
1	1	0	1	-0.5 i_{sl}	-0.5 i_{sl}	0.5 i_{sl}
1	1	0	0	- i_{sl}	- i_{sl}	0
1	0	0	0	- i_{sl}	- i_{sl}	0
0	1	0	0	- i_{sl}	- i_{sl}	0
1	0	1	1	-0.2 i_{sl}	-0.2 i_{sl}	0.8 i_{sl}
0	1	1	1	-0.2 i_{sl}	-0.2 i_{sl}	0.8 i_{sl}
0	0	1	1	0	0	i_{sl}
0	0	1	0	0	0	i_{sl}
0	0	0	1	0	0	i_{sl}
0	0	0	0	Not allowed		

Considering the single-stage LBT, it can be seen from Fig. 5 that two-thirds of the secondary current is supplied by one of the primary windings and the remaining one-third is supplied by the other two primary windings. Meanwhile, the secondary side of the two-stage LBT (see Fig. 7) includes two secondary windings along with four coupling windings per phase as shown by the equivalent circuit in Fig. 8. Five switching states can be found for each phase with which the primary currents can be regulated toward a desirable unbalance level. Hence, considering possible switching states for all three phases, still primary and secondary currents can be described by using $\mathbf{Z}$ in (12), where the values of k_1, k_2, and k_3 can be given as

$$\begin{cases} k_1 = \frac{2s_{11}}{2+s_{12}+C_{11}+C_{12}} + \frac{2s_{12}}{2+s_{11}+C_{11}+C_{12}} \\ k_2 = \frac{2s_{21}}{2+s_{22}+C_{21}+C_{22}} + \frac{2s_{22}}{2+s_{21}+C_{21}+C_{22}} \\ k_3 = \frac{2s_{31}}{2+s_{32}+C_{31}+C_{32}} + \frac{2s_{32}}{2+s_{31}+C_{31}+C_{32}} \end{cases}. \quad (14)$$

Practically, five possible switching states for the four switches per phase makes 125 switching statuses for a three-phase combination in total. Combining (6) and (9) with (12) will result in

$$\begin{bmatrix} I_{P0} \\ I_{P-} \\ I_{P+} \end{bmatrix} = \begin{bmatrix} 3k_1-2 & 3k_2-2 & 3k_3-2 \\ 1 & \alpha^2 & \alpha \\ 1 & \alpha & \alpha^2 \end{bmatrix} \begin{bmatrix} I_{S1} \\ I_{S2} \\ I_{S3} \end{bmatrix}. \quad (15)$$

According to (11), while the original LBT has no effects on positive- and negative-sequence currents, it significantly mitigates the zero-sequence components. This can also be achieved by using conventional delta-star distribution transformers, requiring no extra coupling windings that increase the weight and volume of the transformer. Moreover, according to (15), the addition of extra switches to the original LBT (both single stage

and two stage) not only has no effects on positive- and negative-sequence components, it also imposes zero-sequence components to the primary side of the transformer. These discussed LBTs are only capable of distributing the overload of the secondary phases over the primary phases. In fact, the only advantage of the original as well as the modified LBT is the possibility of releasing the unusable capacity of transformer under overloaded unbalanced conditions compared to the conventional distribution transformer. Hence, the following section examines further modifications to the best LBT in order to compare its improvement in terms of its primary negative-sequence unbalance factor, released capacity of transformers, as well as their costs.

C. Modified Optimal LBT

While the obtained best (optimal) LBT (see Fig. 4) also suffers the lack of control on the primary currents, a multistage proposal can be applied to the best LBT as shown in Fig. 9. Six coupling windings along with six switches are added to the available optimal LBT shown in Fig. 4 in order to achieve a switch-mode single-stage optimal LBT. It is noticeable that the additional parallel branches are essential to control primary currents. At the same time, instantaneous voltages of these branches, which are connected to each secondary phase, have to be equal. Thus, the **CV** of the single-stage optimal LBT can be given as follows:

$$\begin{cases} [1/2,1,0]\|[-1/2,0,-1] \text{ or } (\mathbf{j}+\frac{1}{2}\mathbf{i})\|\,(-\mathbf{k}-\frac{1}{2}\mathbf{i}) \\ [1,0,1/2]\|[0,-1,-1/2] \text{ or } (\mathbf{i}+\frac{1}{2}\mathbf{k})\|\,(-\mathbf{j}-\frac{1}{2}\mathbf{k}) \\ [0,1/2,1]\|[-1,-1/2,0] \text{ or } (\mathbf{k}+\frac{1}{2}\mathbf{j})\|(-\mathbf{i}-\frac{1}{2}\mathbf{j}) \end{cases}. \tag{16}$$

This combination enables the controller to regulate the current through the secondary and coupling windings.

1) Analysis and Operation of the Modified Best LBT: Here, the modified best LBT is suggested to improve the unbalance of primary currents. Assume the turn ratio between the secondary winding and the coupling winding is equal to two. Fig. 9 shows that windings Y_{11} and B_2 are connected through the switch S_{11} to phase 2, Y_{32} and F_2 through the switch S_{32} to phase 2, Y_{12} and B_3 through the switch S_{12} to phase 1, Y_{22} and F_3 through the switch S_{22} to phase 1, windings Y_{21} and B_1 are connected through the switch S_{21} to phase 3, where $\mathrm{Y}_{31}, \mathrm{F}_1$ are connected through the switch S_{31} to phase 3. Thus, when the two switches S_{12} and S_{22} are turned ON and OFF, respectively, the secondary current I_{S1} is supplied through the secondary winding Y_{12} and the coupling winding B_3 by the primary phases a and c; when S_{12} is OFF and S_{22} is ON, the secondary current I_{S1} is supplied through the secondary winding Y_{22} and the coupling winding F_3 by the primary phases b and c; when S_{12} and S_{22} are turned ON, the secondary current I_{S1} is totally supplied through the secondary windings Y_{12} and Y_{22} by the primary phases a and b. This design and analysis can also be generalized to a multistage topology as described earlier in Section III-B for the optimal LBT.

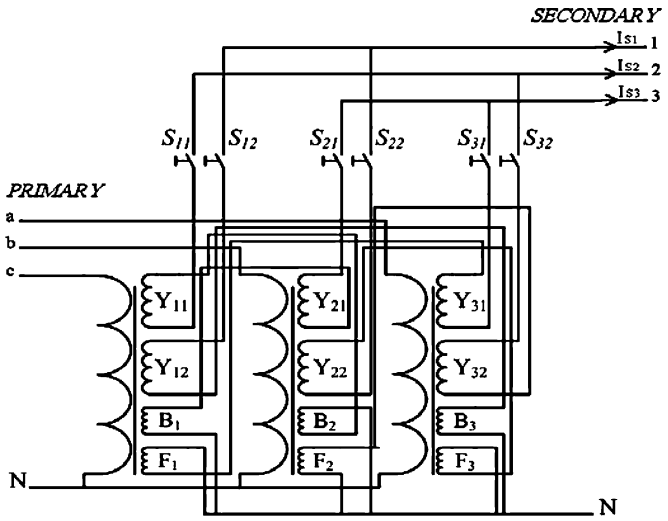

Fig. 9. Single-stage switch-mode proposed topology for the best LBT.

Hence, considering all possible switching statues for the three phases, primary and secondary currents can be related as follows:

$$\begin{bmatrix} I_{Pa} \\ I_{Pb} \\ I_{Pc} \end{bmatrix} = \begin{bmatrix} \frac{S_{12}}{S_{12}+S_{22}} & \frac{-S_{11}}{S_{11}+S_{32}} & 2(S_{21}-S_{31}) \\ \frac{-S_{22}}{S_{12}+S_{22}} & 2(S_{32}-S_{11}) & \frac{S_{21}}{S_{21}+S_{31}} \\ 2(S_{12}-S_{22}) & \frac{S_{32}}{S_{11}+S_{32}} & \frac{-S_{31}}{S_{21}+S_{31}} \end{bmatrix} \times \begin{bmatrix} I_{S1} \\ I_{S2} \\ I_{S3} \end{bmatrix} \tag{17}$$

where I_{Pa}, I_{Pb}, and I_{Pc} are three-phase primary currents; and I_{S1}, I_{S2}, and I_{S3} are three-phase secondary currents. Also, the values of $S_{11}, S_{12}, S_{21}, S_{22}, S_{31}$, and S_{32} are equal to 1 when they are in the ON state, and 0 in the OFF position. Applying the same approach as that given for the modified LBT [see (12)– (15)] to the modified best LBT leads to the following relationship:

While the original and switch-mode LBT were unable to improve the current unbalance factor (CUF) worked out according to the IEEE definition, the modified best LBT is capable of improving the CUF in a flexible manner based on (18), shown at the bottom of the page.

$$\begin{bmatrix} I_{P0} \\ I_{P-} \\ I_{P+} \end{bmatrix} = \begin{bmatrix} \frac{(S_{12}-S_{22})\times 2\left(S_{12}^2-S_{22}^2\right)}{S_{12}+S_{22}} & \frac{(S_{32}-S_{11})\times 2\left(S_{32}^2-S_{11}^2\right)}{S_{11}+S_{32}} & \frac{(S_{21}-S_{31})\times 2(S_{21}^2-S_{31}^2)}{S_{21}+S_{31}} \\ 1+\frac{\alpha\left(S_{22}+2S_{12}^2-2S_{22}^2\right)}{S_{12}+S_{22}} & -1+\frac{\alpha^2(2S_{32}^2-2S_{11}^2-S_{32})}{S_{11}+S_{32}} & -1+\frac{2S_{21}^2-2S_{31}^2-\alpha S_{21}}{S_{21}+S_{31}} \\ 1+\frac{\alpha^2\left(S_{22}+2S_{12}^2-2S_{22}^2\right)}{S_{12}+S_{22}} & -1+\frac{\alpha(2S_{32}^2-2S_{11}^2-S_{32})}{S_{11}+S_{32}} & -1+\frac{2S_{21}^2-2S_{31}^2-\alpha^2 S_{21}}{S_{21}+S_{31}} \end{bmatrix} \begin{bmatrix} I_{S1} \\ I_{S2} \\ I_{S3} \end{bmatrix} \tag{18}$$

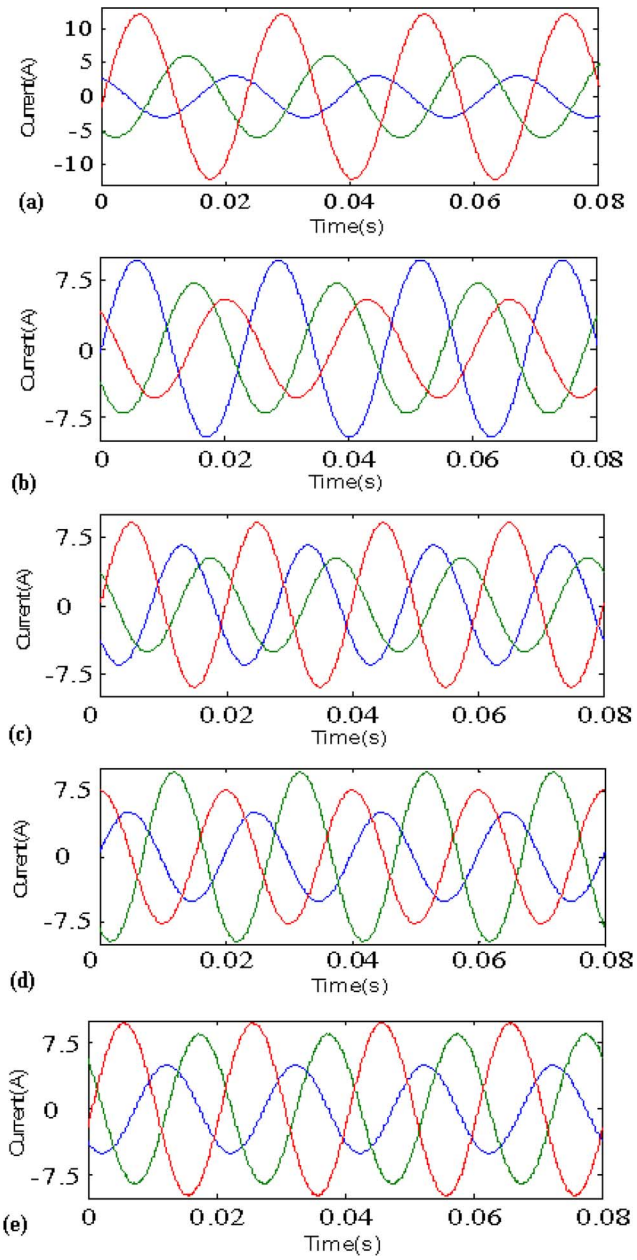

Fig. 10. (a) Simulated secondary-side unbalanced load currents ($3.03e^{-j0.28^\circ}$ (A), $12.09e^{-j120.66^\circ}$ (A), $6.04e^{j119.63^\circ}$ (A)), and resulting primary currents under four different proposed LBT topologies. (b) Original LBT (see Fig. 1: ($10.22e^{-j118.63^\circ}$ (A), $7.88e^{j95.65^\circ}$ (A), $5.78e^{j11.22^\circ}$ (A))). (c) Single-stage switch-mode LBT (see Fig. 6: ($8.78e^{j0.8^\circ}$ (A), $5.56e^{j144.76^\circ}$ (A), $7.98e^{-j144.62^\circ}$ (A))). (d) Two-stage switch-mode LBT (see Fig. 7: ($6.09e^{j90.57^\circ}$ (A), $10.16e^{-j113.83^\circ}$ (A), $5.5e^{j5.83^\circ}$ (A))). (e) Switch-mode optimal LBT (see Fig. 9: ($5.52e^{j221.8^\circ}$ (A), $8.48e^{j102.57^\circ}$ (A), $9.58e^{-j12.78^\circ}$ (A))).

IV. Typical Simulations

Assume three single-phase resistive loads (66 Ω, 16.5 Ω, and 33 Ω) are connected to secondary-side phases 1, 2, and 3. This three-phase load combination consumes purely active power, where no pure reactive compensators (neither switch-mode nor passive inductors/capacitors) are capable of distributing pure active power among the three phases directly. Further, the values of unbalanced resistors are identical for both simulations and experimental work. Four different simulations are arranged with MATLAB in which the unbalanced load is examined by using the original LBT (Fig. 1), the single-stage switch-mode LBT (Fig. 6), the multistage switch-mode LBT (Fig. 7) and the switch-mode optimal LBT (Fig. 9). Fig. 10(a) shows the three-phase unbalanced load currents. It can be seen from Table IV that the magnitude of the unbalance factor for the load currents ($Mag = [(I_-/I_1)^2 + (I_0/I_1)^2]^{1/2}$) is 53.45% calculated based on the IEEE definitions [19], and 26.79% based on the NEMA definition [20] (excluding zero-sequence unbalance). Also, the released capacity (RC) of the four designs is calculated based on the formulation given in [21]

$$RC\% = \frac{3\max(p_a, p_b, p_c) - \sum_{j=a,b,c} p_j}{3\max(p_a, p_b, p_c)} \times 100. \qquad (19)$$

Then, using the concept of mutual inductances in [22], four different simulations were performed to look into the performances of the four different LBTs, concentrating on reducing the unbalance of primary currents. Fig. 10(b) introduces simulations for the original LBT, Fig. 10(c) those of the single-stage switch-mode LBT, Fig. 10(d) those of the two-stage switch-mode LBT, and Fig. 10(e) for those of the single-stage switch-mode optimal LBT. Table IV lists the resulting unbalance factors of the four LBTs using the IEEE and NEMA definitions. The efficiency (η), the released capacity (RC), and the calculated unbalance percents show some facts about various examined LBTs in comparison with the available load unbalance percent as follows.

- The original LBT cancels zero-sequence currents, having no effect on the negative-sequence component.
- The proposed single-stage and two-stage switch-mode topologies make the unbalance even worse than the original LBT.

TABLE IV
Simulated Range of RC, CUF, and Efficiency for Different LBTs

	Released Capacity	NEMA Standard	IEEE standard			η (%)
	RC%	Excluding zero sequence	$\lvert I_-\rvert/\lvert I_+\rvert$ (%)	$\lvert I_0\rvert/\lvert I_+\rvert$ (%)	*Mag* (%)	
Load	_	26.79	37.80	37.80	53.45	-
Original LBT	18.46	26.79	37.80	0	37.80	99.4
Best LBT (Zig-zag)	19.15	26.79	35.9	0	35.9	99.5
One-stage Switch-Mode LBT	27.37	26.79	37.80	12.30	39.70	99.3
Two-stage Switch-Mode LBT	18.96	26.79	37.80	15.12	40.70	98.8
Switch-Mode Best LBT	27.76	11.16	12.80	23.29	26.57	99.1

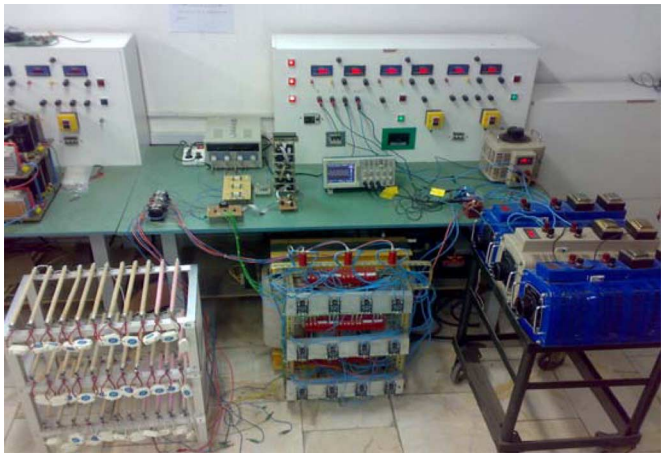

Fig. 11. Developed modular design of the LBT for practical examination of the four various cases.

TABLE V
EXPERIMENTAL COMPARISONS OF RC AND CUF FOR DIFFERENT LBTS

	Released Capacity	NEMA Standard	IEEE standard		
	RC%	Excluding zero sequence	$\lvert I_-\rvert/\lvert I_+\rvert$ (%)	$\lvert I_0\rvert/\lvert I_+\rvert$ (%)	*Mag* (%)
Load	_	27.81	42.02	34.34	54.27
Original LBT	18.16	27.47	40.01	6.87	40.59
One-stage Switch-Mode LBT	27.33	26.23	37.01	10.97	38.6
Two-stage Switch-Mode LBT	18.16	30.62	41.76	12.31	43.54
Switch-Mode Best LBT	27.33	11.64	12.17	14.75	19.12

- The single-stage switch-mode best LBT not only lowers zero sequence, but also lowers the negative-sequence component of the primary currents.
- The magnitude of the IEEE unbalance percent ($Mag\%$) for the switch-mode best LBT proposal is much better than other examined cases.
- The released capacity of the switch-mode best LBT is higher than other examined cases.
- The high efficiency of the switch-mode best LBT is lower than the original LBT of about 0.3%.
- The best LBT (see Fig. 4) was also simulated, showing somehow better performance than the original LBT (see the third case in Table IV).

V. EXPERIMENTAL VALIDATION

To verify the detailed performed analysis and simulations on the proposed LBT and the original LBT (Fig. 1), both single and two-stage switch-mode LBTs (Figs. 6 and 7) and the switch-mode optimal LBT (Fig. 9) topologies were implemented as shown in Fig. 11. This three-phase prototype is rated at 12 kVA, 380 V (20 A). The prototype is a modulated design in which seven windings per branch (one input along with six center-tapped ($\sqrt{3}:1$) output windings) were located on each arm (for a total of 21 windings). Then, the required number of windings were used to connect each of the four studied designs according to the proposed LBT. Twelve switches enable the modulated design to be arranged in various kinds of the four examined LBTs listed by Table V. The switches are electrical type solid state, which are triggered with a dc voltage (18 V for ON state, and below 3.5 V for the OFF state). Also, a three-phase load was designed in which the VA of each phase can be regulated by simple switches. Hence, unbalanced three-phase loads can be applied to the LBT by adjusting the developed load.

An unbalanced three-phase condition was arranged by using the developed load in which three resistances of 66 Ω, 16.5 Ω, and 33 Ω (similar to those of the simulations) were connected to secondary-side phases 1, 2, and 3 of the laboratory prototype, respectively. The unbalanced three-phase load currents are shown in Fig. 12(a). Then, four different experiments were arranged, connecting the unbalanced three-phase load to the original LBT (Fig. 1), the single-stage switch-mode LBT (Fig. 6), the two-stage switch-mode LBT (Fig. 7), and the proposed single-stage switch-mode optimal LBT (Fig. 9).

Fig. 12(b) introduces the resulting three-phase primary currents for the original LBT. One advantage is that the biggest magnitude in the primary side is smaller than that of the secondary side [shown in Fig. 12(a)]; but, the primary-side phase differences are bigger than those of the secondary side. Practical outcomes of the primary side of the single-stage switch-mode LBT are shown in Fig. 12(c), releasing higher capacity for the switch-mode single-stage LBT compared to that of the original LBT. The magnitude of the IEEE CUF is higher for the primary side of the single-stage switch-mode LBT than that of the original LBT (see Table V). Note that six switches are added to the one-stage switch-mode LBT. Fig. 12(d) demonstrates the resulting three-phase primary currents of the two-stage switch-mode LBT. Once again, the CUF has not improved despite the addition of several windings along with 12 switches to the secondary side of the LBT. However, the released capacity of this topology is higher than the other two LBTs [see Fig. 12(b) and (c) and Table V].

The last picture, Fig. 12(e), depicts practical outcomes of the primary side of the single-stage switch-mode best LBT. This optimal topology improves the IEEE CUF as well as that of the NEMA. Interestingly, it affects negative- and zero-sequence components unlike the other three examined LBTs. Also, the phase-angle balance between the three phases is improved compared to other topologies. Practical results verify the optimal switch-mode LBT as the best examined LBT under unbalanced conditions. Experimental results shown in Figs. 12(a)–(e) (each vertical unit is equal to 2.88 A) can also be compared with those of the related simulations illustrated by Figs. 10(a)–(e). Table V summarizes the experimental calculated released capacity, the unbalance factor, and efficiencies of different LBTs in comparison with those of Table IV.

Furthermore, the number of windings and turns as well as the volume of different suggested switching-mode LBTs can be compared for the developed prototype accordingly. Assume the apparent power and the magnetic flux density are equal to 12 kVA and 1.2 Tesla, respectively. Then, using the worked out

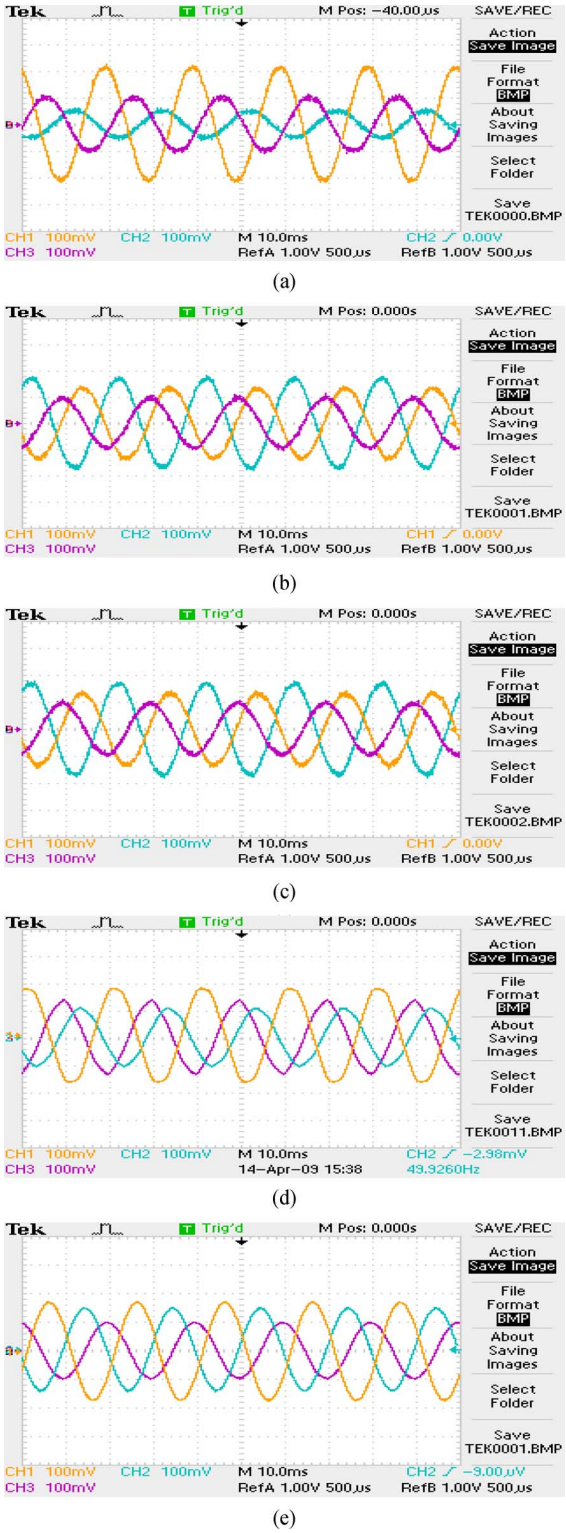

Fig. 12. (a) Unbalanced load currents, and experimental primary currents when applying the unbalanced load to (b) the original LBT (Fig. 1), (c) the single-stage switch-mode LBT (Fig. 6), (d) the two-stage switch-mode LBT (Fig. 7), and (e) the single-stage switch-mode best LBT (Fig. 9).

cross-sectional area of the core (7.5×12 cm^2), 50 Hz, and the electromotive force (emf) equivalent to 220 V, the number of turns for primary windings was calculated to be equal to 92. Then, using a 1:1 turn ratio (for the laboratory prototype), the other six secondary and coupling windings also have 92 turns (each center-taped at 55 turns like the ratio $\sqrt{3}:1$). Tables VI and VII present the number of turns for the primary, secondary, and coupling windings (NT_p, NT_s, and NT_c), dimensions of various LBTs as well as the number of windings wound for the primary, secondary, and coupling windings (NW_p, NW_s, and NW_c) for a conventional distribution transformer, an original LBT, the single stage, the two-stage LBT, and the switch-mode optimal LBT. It can be seen from Table VI that the switch-mode LBT is heavier than the ordinary distribution transformer. The best switch-mode LBT, however, is the lightest transformer among all proposed LBTs. Comparing the volumes of the transformers in Table VII shows that the conventional transformer introduces the lowest volume followed by the switch-mode best LBT. The last column compares the cost of implementing various LBTs, showing the switch-mode best LBT followed by the original LBT as the two lowest costs.

TABLE VI
NUMBER OF WINDINGS AND THEIR TURNS FOR THE EXAMINED TRANSFORMERS

	NW_P	NW_S	NW_C	NT_P	NT_S	NT_C
Ordinary Transformer	**3**	**3**	**0**	**20000**	**380**	**0**
Original LBT	**3**	**3**	**6**	**20000**	**380**	**380**
One-Stage Switch-Mode LBT	**3**	**3**	**6**	**20000**	**380**	**380**
Two-Stage Switch-Mode LBT	**3**	**6**	**12**	**20000**	**380**	**380**
Best Switch-Mode LBT	**3**	**6**	**6**	**20000**	**224**	**112**

TABLE VII
PHYSICAL DIMENSIONS AND COST OF VARIOUS EXAMINED LBTS

	Height (m)	Length (m)	Width (m)	Volume (m^3)	Cost ($)
Ordinary Transformer	0.4056	0.68	0.16	0.04413	1158
Original LBT	0.5368	0.68	0.16	0.05840	1553
One-stage Switch-Mode LBT	0.5368	0.68	0.16	0.05840	1694
Two-Stage Switch-Mode LBT	0.7	0.68	0.16	0.07616	2257
Best Switch-Mode LBT	0.4702	0.68	0.16	0.05116	1504

VI. CONCLUSION

An original LBT can improve the unbalance of distribution systems despite one disadvantage that the distribution of primary currents cannot be properly balanced by the secondary

currents. This paper proposes the addition of several switches to the original LBT that are located on the secondary and coupling windings. A microcontroller can be programmed to select the best possible switching status for balancing purposes. Furthermore, the number of secondary windings is added by introducing a multistage switch-mode LBT. Proposed LBTs are then analyzed and compared with the original LBT. Then, the concept of the LBT is generalized in order to obtain all possible configurations for the LBT. It is shown that the best LBT can be analytically derived among all introduced LBTs. Simulations related to the original LBT are compared with those of the switch-mode LBT and the optimal LBT accordingly. To put the analysis and simulations on a firmer basis, a 12-kVA fundamental structure transformer was implemented as a laboratory prototype. Four various studied LBTs are then tested one by one on the developed modular prototype, introducing the capability of each suggested topology on the balancing issue. Experimental outcomes confirm the analysis and the performed simulations, verifying the optimal switch-mode LBT as the best balancing configuration for distribution substations.

APPENDIX

Fig. 3 illustrates 15 $\mathbf{CV}$s, where four $\mathbf{CV}$s are shown in (2)–(5). Here, another 11 $\mathbf{CV}$s, related to those of Fig. 3, are listed as follows:

$$\begin{cases} [1,1,-1] \text{ or } (\mathbf{i}+\mathbf{j}-\mathbf{k}) \\ [1,-1,1] \text{ or } (\mathbf{i}+\mathbf{k}-\mathbf{j}) \\ [-1,1,1] \text{ or } (\mathbf{j}+\mathbf{k}-\mathbf{i}) \end{cases}$$

$$\begin{cases} [1,1,-1]\|\|[1,1,-2] \text{ or } (\mathbf{i}+\mathbf{j}-\mathbf{k})\|\|(\mathbf{i}-2\mathbf{k}+\mathbf{j}) \\ [1,-1,1]\|\|[1,-2,1] \text{ or } (\mathbf{i}+\mathbf{k}-\mathbf{j})\|\|(\mathbf{i}-2\mathbf{j}+\mathbf{k}) \\ [-1,1,1]\|\|[-2,1,1] \text{ or } (\mathbf{j}+\mathbf{k}-\mathbf{i})\|\|(\mathbf{j}+\mathbf{k}-2\mathbf{i}) \end{cases}$$

$$\begin{cases} [1,1,-1]\|\|[1,1,-2]\|\|[0,0,-1] \text{ or } (\mathbf{i}+\mathbf{j}-\mathbf{k})\|\|(\mathbf{i}-2\mathbf{k}+\mathbf{j})\|\|(-\mathbf{k}) \\ [1,-1,1]\|\|[1,-2,1]\|\|[0,-1,0] \text{ or } (\mathbf{i}+\mathbf{k}-\mathbf{j})\|\|(\mathbf{i}-2\mathbf{j}+\mathbf{k})\|\|(-\mathbf{j}) \\ [-1,1,1]\|\|[-2,1,1]\|\|[-1,0,0] \text{ or } (\mathbf{j}+\mathbf{k}-\mathbf{i})\|\|(\mathbf{j}+\mathbf{k}-2\mathbf{i})\|\|(-\mathbf{i}) \end{cases}$$

$$\begin{cases} [0,1,-2] \text{ or } (\mathbf{j}-2\mathbf{k}) \\ [1,-2,0] \text{ or } (\mathbf{i}-2\mathbf{j}) \\ [-2,0,1] \text{ or } (\mathbf{k}-2\mathbf{i}) \end{cases}$$

$$\begin{cases} [1,-1,-1]\|\|[1,0,0] \text{ or } (\mathbf{i}-\mathbf{j}-\mathbf{k})\|\|(\mathbf{i}) \\ [-1,-1,1]\|\|[0,0,1] \text{ or } (\mathbf{k}-\mathbf{i}-\mathbf{j})\|\|(\mathbf{k}) \\ [-1,1,-1]\|\|[0,1,0] \text{ or } (\mathbf{j}-\mathbf{k}-\mathbf{i})\|\|(\mathbf{j}) \end{cases}$$

$$\begin{cases} [2,-1,-1]\|\|[1,0,0] \text{ or } (2\mathbf{i}-\mathbf{j}-\mathbf{k})\|\|(\mathbf{i}) \\ [-1,-1,2]\|\|[0,0,1] \text{ or } (2\mathbf{k}-\mathbf{i}-\mathbf{j})\|\|(\mathbf{k}) \\ [-1,2,-1]\|\|[0,1,0] \text{ or } (2\mathbf{j}-\mathbf{k}-\mathbf{i})\|\|(\mathbf{j}) \end{cases}$$

$$\begin{cases} [\frac{\sqrt{3}}{2}, 1+\frac{\sqrt{3}}{2}, -1-\frac{\sqrt{3}}{2}]\|\|[0,1,-2] \text{ or } ((\mathbf{j}-\mathbf{k})+\frac{\sqrt{3}}{2}(\mathbf{i}+\mathbf{j}-\mathbf{k}))\|\|(\mathbf{j}-2\mathbf{k}) \\ [1+\frac{\sqrt{3}}{2}, -1-\frac{\sqrt{3}}{2}, \frac{\sqrt{3}}{2}]\|\|[1,-2,0] \text{ or } ((\mathbf{i}-\mathbf{j})+\frac{\sqrt{3}}{2}(\mathbf{i}+\mathbf{k}-\mathbf{j}))\|\|(\mathbf{i}-2\mathbf{j}) \\ [-1-\frac{\sqrt{3}}{2}, \frac{\sqrt{3}}{2}, 1+\frac{\sqrt{3}}{2}]\|\|[-2,0,1] \text{ or } ((\mathbf{k}-\mathbf{i})+\frac{\sqrt{3}}{2}(\mathbf{j}+\mathbf{k}-\mathbf{i}))\|\|(\mathbf{k}-2\mathbf{i}) \end{cases}$$

$$\begin{cases} [-1,4,-1]\|\|[-1,2,-1]\|\|[0,1,0] \text{ or } (4\mathbf{j}-\mathbf{i}-\mathbf{k})\|\|(2\mathbf{j}-\mathbf{i}-\mathbf{k})\|\|(\mathbf{j}) \\ [-1,-1,4]\|\|[-1,-1,2]\|\|[0,0,1] \text{ or } (4\mathbf{k}-\mathbf{i}-\mathbf{j})\|\|(2\mathbf{k}-\mathbf{i}-\mathbf{j})\|\|(\mathbf{k}) \\ [4,-1,-1]\|\|[2,-1,-1]\|\|[1,0,0] \text{ or } (4\mathbf{i}-\mathbf{j}-\mathbf{k})\|\|(2\mathbf{i}-\mathbf{j}-\mathbf{k})\|\|(\mathbf{i}) \end{cases}$$

$$\begin{cases} [0,2,-1] \text{ or } (2\mathbf{j}-\mathbf{k}) \\ [-1,0,2] \text{or} (2\mathbf{k}-\mathbf{i}) \\ [2,-1,0] \text{ or } (2\mathbf{i}-\mathbf{j}) \end{cases}$$

$$\begin{cases} [-1,1,-1] \text{ or } (\mathbf{j}-\mathbf{i}-\mathbf{k}) \\ [1,-1,-1] \text{ or } (\mathbf{i}-\mathbf{k}-\mathbf{j}) \\ [-1,-1,1] \text{ or } (\mathbf{k}-\mathbf{j}-\mathbf{i}) \end{cases}$$

$$\begin{cases} [0,2,0]\|\|[-1,1,-1] \text{ or } (\mathbf{j}-\mathbf{i}-\mathbf{k})\|\|(2\mathbf{j}) \\ [2,0,0]\|\|[1,-1,-1] \text{ or } (\mathbf{i}-\mathbf{k}-\mathbf{j})\|\|(2\mathbf{i}) \\ [0,0,2]\|\|[-1,-1,1] \text{ or } (\mathbf{k}-\mathbf{j}-\mathbf{i})\|\|(2\mathbf{k}) \end{cases}$$

ACKNOWLEDGMENT

Experimental works were performed in reactive power control and power quality Laboratory of K. N. Toosi University of technology. The authors would like to thank the efforts made by related officials.

REFERENCES

[1] E. A. Donohue, "System and Method of Load Balancing Using Fuzzy Logic," U.S. Patent 0 168 463 A1, Jul. 10, 2008.

[2] S. Y. Lee and C. J. Wu, "Reactive power compensation and load-balancing for unbalanced three-phase four-wire system by a combined system of an SVC and a series active filter," *Proc. Inst. Elect. Eng., Elect. Power Appl.*, vol. 147, no. 6, pp. 563–578, Nov. 2000.
[3] T. J. E. Miller, *Reactive Power Control in Electric System*. New York: Wiley, 1982.
[4] Z. Yongqiang and L. Wenhua, "Balancing compensation of unbalanced load based on single phase STATCOM," in *Proc. IPEMC Power Electronics and Motion Control Conf.*, Aug. 2004, vol. 2, pp. 425–429.
[5] B. N. Singh, B. Singh, A. Chandra, and K. Al-Haddad, "Digital implementation of an advanced static compensator for voltage profile improvement, power-factor correction and balancing of unbalanced reactive loads," *Elect. Power Syst. Res.*, vol. 54, pp. 101–111, May 2000.
[6] A. Sonnenmoser and P. W. Lehn, "Line current balancing with a unified power flow controller," *IEEE Trans. Power Del.*, vol. 14, no. 3, pp. 1151–1157, Jul. 1999.
[7] J. H. Chen, W. J. Lee, and M. S. Chen, "Using a static var compensator to balance a distribution system," *IEEE Trans. Ind. Appl.*, vol. 35, no. 2, pp. 298–304, Mar./Apr. 1999.
[8] S. Y. Lee, C. J. Wu, and W. N. Chang, "A compact control algorithm for reactive power compensation and load-balancing with static var compensator," *Elect. Power Syst. Res.*, vol. 58, pp. 63–70, Jun. 2001.
[9] M. T. Bina and A. K. S. Bhat, "Averaging technique for the modeling of STATCOM and active filters," *IEEE Trans. Power Electron.*, vol. 23, no. 2, pp. 723–734, Mar. 2008.
[10] V. B. Bhavaraju and P. N. Enjeti, "Analysis and design of an active power filter for balancing unbalanced loads," *IEEE Trans. Power Electron.*, vol. 8, no. 4, pp. 640–647, Oct. 1993.
[11] A. Chandra, B. Singh, B. N. Singh, and K. Al-Haddad, "An improved control algorithm of shunt active filter for voltage regulation, harmonic elimination, power-factor correction and balancing of nonlinear loads," *IEEE Trans. Power Electron.*, vol. 15, no. 3, pp. 495–507, May 2000.
[12] M. T. Bina and E. Pashajavid, "An efficient procedure to design passive LCL-filters for active power filters," *Elect. Power Syst. Res.*, vol. 79, no. 4, pp. 606–614, Nov. 2008.
[13] C. C. Chen and Y. Y. Hsu, "A novel approach to the design of a shunt active filter for an unbalanced three-phase four-wire system under nonsinusoidal conditions," *IEEE Trans. Power Del.*, vol. 15, no. 4, pp. 1258–1264, Oct. 2000.
[14] M. T. Bina and D. C. Hamill, "Average circuit model for angle-controlled STATCOM," *Proc. Inst. Elect. Eng., Elect. Power Appl.*, vol. 152, no. 3, pp. 653–659, May 2005.
[15] T. J. Reynal, "Load-Balancing Transformer," U.S. Patent 5 557 249, Sep. 1996.
[16] J. D. Glover and M. Sarma, *Power System Analysis and Design*, 2nd ed. Pacific Grove, CA: PWS Publishing , 1994.
[17] Y.-J. Wang and M.-J. Yang, "Probabilistic modeling of three-phase voltage unbalance caused by load fluctuations," in *Proc. IEEE Power Eng. Soc. Winter Meeting*, 2000, vol. 4, pp. 2588–2593.
[18] C. L. Fortescue, "Method of symmetrical coordinates applied to the solution of polyphase networks," *Trans. ALEE*, vol. 37, pp. 1027–1140, 1918.
[19] A. von Jouanne and B. B. Banerjee, "Assessment of voltage unbalance," *IEEE Trans. Power Del.*, vol. 16, no. 4, pp. 782–790, Oct. 2001.
[20] *Motors and Generators*, NEMA Std. MG 1-1993.
[21] M. T. Bina, "Over-capacity of distribution transformers under unbalanced condition," in *Proc. 24th Int. Power System Conf.*, Tehran, Iran, 2009, vol. 1, pp. 1–8.
[22] J. Wang, A. F. Witulski, J. L. Vollin, T. K. Phelps, and G. I. Cardwell, "Derivation, calculation and measurement of parameters for a multi-winding transformer electrical model," in *Proc. Applied Power Electronics Conf. Expo.*, Mar. 1999, vol. 1, pp. 220–226.

D. Ahmadi was born in Tehran, Iran, in 1985. He received the B.Sc. degree in electrical engineering from the Zanjan University in 2007 and the M.Sc. degree in power engineering and power quality from K. N. Toosi University of Technology, Tehran, in 2009.

M. Tavakoli Bina (S'98–M'01–SM'07) received the B.Sc. and M.Sc. degrees n power electronics and power system utility applications from the University of Tehran and Ferdowsi in 1988 and 1991, respectively, and the Ph.D. degree from the University of Surrey, Guildford, U.K., in 2001.

From 1992 to 1997, he was Lecturer working on power systems with the K. N. Toosi University of Technology, Tehran. He joined the Faculty of Electrical and Computer Engineering at K. N. Toosi University of Technology in 2001, where he is currently an Associate Professor of Electrical Engineering and is engaged in teaching and conducting research in the area of power electronics and utility applications. While he is currently Head of the Department of Power Engineering at the K. N. Toosi University of Technology, he has been responsible for the development of flexible power systems, power-quality, and power-electronics courses, and laboratories in the Faculty of Electrical and Computer Engineering.

Dr. Bina is a registered professional engineer in the Province of Tehran.

M. Golkar was born in Tehran, Iran, in 1954. He received the B.Sc. degree in electrical engineering (power systems) from the Sharif University of Technology, Tehran, Iran, in 1977, the M.Sc. degree from the Oklahoma State University, Stillwater, in 1979, and the Ph.D. degree from the Imperial College of Science, Technology, and Medicine (The University of London), London, U.K., in 1986.

His employment experience included working at K. N. Toosi University, Tehran, in 1979 and Advisor to the Tehran Electricity Board, Shiraz Electricity Board, and Bandar Abbas Electricity Board in the field of distribution systems. He is Head of the Research Group at the Electric Power Research Center in the field of reactive power control and distribution system studies from 1987 to 1997 and Senior Lecturer at the Curtin University of Technology, Malaysia, from 2002 to 2005.